Plasma wave instability and amplification of terahertz radiation in field-effect-transistor arrays



2008 J. Phys.: Condens. Matter 20 384208

(http://iopscience.iop.org/0953-8984/20/38/384208)

J. Phys.: Condens. Matter **20** (2008) 384208 (6pp) doi:10.1088/0953-8984/20/38/384208

# Plasma wave instability and amplification of terahertz radiation in field-effect-transistor arrays

**V V Popov[1], G M Tsymbalov[1] and M S Shur[2]**

[1] Institute of Radio Engineering and Electronics (Saratov Branch), Russian Academy of Sciences, 410019 Saratov, Russia
[2] Department of Electrical, Computer, and System Engineering and Center for Integrated Electronics, C119015, Rensselaer Polytechnic Institute, Troy, NY 12180, USA

Received 7 March 2008, in final form 24 April 2008
Published 21 August 2008
Online at stacks.iop.org/JPhysCM/20/384208

**Abstract**
We show that the strong amplification of terahertz radiation takes place in an array of field-effect transistors at small DC drain currents due to hydrodynamic plasmon instability of the collective plasmon mode. Planar designs compatible with standard integrated circuit fabrication processes and strong coupling of terahertz radiation to plasmon modes in FET arrays make such arrays very attractive for potential applications in solid-state terahertz amplifiers and emitters.

## Introduction

Unstable plasma oscillations (plasmons) in field-effect transistors (FETs) with two-dimensional (2D) electron channels can be used for the generation of terahertz (THz) radiation [1]. Hydrodynamic instability of plasmons in the 2D channel of a FET with a single gate was predicted in [2]. This instability type develops at small electron drift velocities (which might be much less than the plasmon phase velocity) if asymmetrical boundary conditions for plasmons are realized at different ends of the gated portion of the 2D electron channel, such as a short-circuit condition at the source and an open-circuit condition at the drain ends of the gated section of the channel. Alternatively, large drain currents close to the saturation regime may produce needed asymmetry of the channel [3]. THz emission linked to unstable plasmons in different FET structures was reported in several papers [3–5]. This type of plasmonic instability advantageously differs from the Cherenkov-like plasmon instability in the grating-gated 2D electron structure, where the electron DC drift velocity has to exceed the grating-coupled-plasmon phase velocity [6–8].

References [1–5] did not address the important problem of coupling the unstable plasmons to THz radiation. The gated plasmons, in general, couple very poorly to THz radiation due to an acoustical nature and, hence, small net dipole moment of this plasmon mode [9] so that special antennas are needed to couple the gated plasmons to THz radiation. This is consistent with the very small output THz emission power (of nanowatt level or less) observed in experiments [3–5] without using special coupling elements.

In an earlier paper [10], it was suggested that the coupling between plasmons in the FET channel and THz radiation might be more effective if FET units were arranged in an array. In our recent paper [11], we showed that the enhancement of the coupling grows proportionally to the number squared of the FET units in the array due to the formation of a collective plasmon mode delocalized over the entire FET array. Coupling of the gated plasmons in the FET array to THz radiation also dramatically improves because the charge distributions in the gate and side contacts have the same symmetry as excited by both the gated plasmon mode or by THz radiation [11]. Because of that, the FET array acts as an aerial matched antenna coupling the plasmons to the THz radiation.

In this paper, we theoretically study the amplification of THz radiation in a one-dimensional planar FET array and show that strong amplification takes place at relatively small DC drain currents due to the hydrodynamic plasmon instability. In section 1, we obtain the expression for the conductivity of the drifting 2D electron fluid confined in a spatially periodic FET array. The electromagnetic approach that we use to calculate THz absorption and amplification in the FET array is described in section 2. In section 3, we discuss the plasmonic and THz amplification properties of the FET array. The conclusions are summarized in section 4.

 

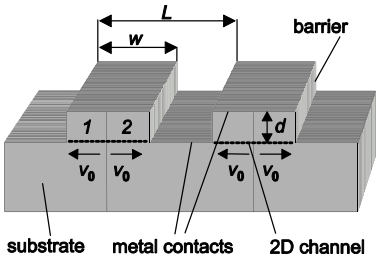


**Figure 1.** Schematic diagram of the FET array. Incoming THz radiation is incident normally from the top.

## 1. High-frequency conductivity of drifting 2D electron fluid in the planar FET array

We consider a field-effect-transistor array with isolated 2D electron channels and conjugate side contacts of adjacent FET units (figure 1). An external THz wave is incident upon the FET array in the normal direction to the FET array plane. The terahertz amplification takes place due to the hydrodynamic instability of plasma waves developed in the FET channels. In the FET array shown in figure 1, the boundary conditions at the source and drain ends of the channel in each FET unit are symmetrical because of the planar geometry of the FET array. The condition for the plasmon instability is ensured by the excitation of specific plasmon modes in the FET array. The incoming THz wave with the electric field polarized across the FET array (in the $x$-direction) induces antisymmetrical vertical electric field under the source and drain edges of the gate contacts in each FET unit. This electric field excites plasmon modes with the nodes of the vertical component of the oscillating electric field under the centers of the gate contacts. It means that one has the short-circuited condition for the vertical electric field under the center of the gate contact, while there are close-to-open-circuited conditions at the edges of the gate contact in each FET unit. To ensure the plasmon instability in such a device, one has to use oppositely applied DC drain currents in sections 1 and 2 of the FET unit (we assume that counter-directed DC electron drift velocities have the same value in each of the two half-sections of the FET unit, see figure 1). To achieve that, an additional current carrying contact is added to the device channel in the middle between the two contacts shown in figure 1. (This contact at the center of the FET unit channel is not shown in figure 1.) In this sense each FET unit in the array is similar to two identical single-gate FETs with combined gates and merged source contacts, which are short-circuited in the center of the FET unit. Depending on biasing, the electron velocity direction opposite to that in figure 1 could also be obtained.

The entire set of electron channels in the FET array (which is infinite in our theoretical model) can be considered as a single conductive plane with a spatially periodic (with period $L$) electron density and DC electron drift velocities. The most general linear expression for the electric current with surface density $J(x,0)$ induced in a spatially modulated 2D electron system located in the plane $y = 0$ by the oscillating electric field $E(x,y,t) = E(x,y)\exp(-\mathrm{i}\omega t)$ is (harmonic time-dependence is omitted)

$$J(x,0) = \int_{-\infty}^{\infty} \sigma(x,x')E(x',0)\,\mathrm{d}x', \tag{1}$$

where the kernel $\sigma(x,x')$ describes the spatial dispersion in the 2D electron system. In a spatially periodic system with period $L$ along the $x$-coordinate, the electric field $E(x,y)$ has spatially periodic amplitude

$$E(x,y) = \sum_{m=-\infty}^{\infty} E_m(y)\exp(\mathrm{i}q_m x), \tag{2}$$

where $E_m(y)$ is the amplitude of the Fourier-harmonic of the electric field having an in-plane wavevector $q_m = 2\pi m/L$, with $m$ being an integer. Substituting equation (2) into equation (1) yields

$$J(x,0) = \sum_{m=\infty}^{\infty} \sigma_m(x)E_m(0)\exp(\mathrm{i}q_m x) \tag{3}$$

with the conductivity function

$$\sigma_m(x) = \int_{-\infty}^{\infty} \sigma(x,x')\exp[\mathrm{i}q_m(x'-x)]\,\mathrm{d}x'.$$

Ohm's law in the form of equation (3) accounts for a spatial periodicity of the FET array and also for the spatial dispersion of the conductivity of the 2D electron system arising from (counter-directed) DC electron drift in different half-sections of each FET unit.

An explicit expression for the conductivity function $\sigma_m(x)$ can be found assuming a certain physical model, either the kinetic or hydrodynamic one, describing the electron dynamics in a 2D electron system. We describe the electron motion in a spatially periodic 2D electron channel and side metal contacts of the FET array by the Euler equation

$$\frac{\mathrm{d}}{\mathrm{d}x}\left[V_0(x)\tilde{V}(x)\right] + (\nu - \mathrm{i}\omega)\tilde{V}(x) = -\frac{e}{m}\sum_{m=-\infty}^{\infty} E_m(0)\exp(\mathrm{i}q_m x) \tag{4}$$

and the continuity equation

$$\frac{\mathrm{d}}{\mathrm{d}x}\left[V_0(x)\tilde{N}(x)\right] - \mathrm{i}\omega\tilde{N}(x) = -\frac{\mathrm{d}}{\mathrm{d}x}\left[N_0(x)\tilde{V}(x)\right], \tag{5}$$

where $N_0(x)$ and $V_0(x)$ are the equilibrium sheet electron density and DC electron drift velocity, respectively, $\tilde{N}(x)$ and $\tilde{V}(x)$ are the amplitudes of the oscillating 2D electron density and electron velocity in the FET channel, $E_m(0)$ is the amplitude of the Fourier-harmonic of the in-plane oscillating electric field in the plane of the 2D electron channel, $e$ and $m$ are the electron charge ($e < 0$) and effective mass, respectively, and $\nu$ is the electron momentum relaxation rate. All the variables in equations (4) and (5) are periodic functions of the $x$-coordinate with period $L$.

Let us rewrite equations (4) and (5) in the canonical forms

$$\frac{\mathrm{d}\psi_V}{\mathrm{d}x} + s_1(x)\psi_V(x) = g_1(x), \tag{6}$$

$$\frac{\mathrm{d}\psi_N}{\mathrm{d}x} + s_2(x)\psi_N = g_2(x), \tag{7}$$

for functions $\psi_V(x) = V_0(x)\tilde{V}(x)$,and $\psi_N(x) = V_0(x)\tilde{N}(x)$, respectively, where

$$s_1(x) = \frac{\nu - \mathrm{i}\omega}{V_0(x)}, \qquad s_2(x) = -\frac{\mathrm{i}\nu}{V_0(x)},$$
$$g_1(x) = \frac{e}{m}\sum_{m=-\infty}^{\infty} E_m(0)\exp(\mathrm{i}q_m x),$$
$$g_2(x) = -\frac{\mathrm{d}}{\mathrm{d}x}\left[\frac{N_0(x)}{V_0(x)}\psi_V(x)\right].$$

Both equations (6) and (7) are differential equations of first order with variable coefficients of the form

$$\frac{\mathrm{d}f}{\mathrm{d}x} + \varphi_1(x)f(x) = \varphi_2(x)$$

for a function $f(x)$ defined in the interval $a \leqslant x \leqslant b$. The general solution of this equation is

$$f(x) = \exp\left(-\int_a^x \varphi_1(x')\,\mathrm{d}x'\right)\left[f(a) + \int_a^x \varphi_2(x') \times \exp\left(\int_a^x \varphi_1(x')\mathrm{d}x'\right)\mathrm{d}x'\right]. \tag{8}$$

We assume a rectangular profile of the equilibrium sheet electron density distribution in a 2D electron channel plane over the period of the FET array: $N_0(x) = N_{2D}$ in either half-section 1 and 2 of the FET unit channel and $N_0(x) = N_M$ in the side contacts. The DC electron drift velocities are $V_0^{(1)}$ and $V_0^{(2)}(V_0^{(1)} = -V_0^{(2)})$ in half-sections 1 and 2 of the FET unit channel, respectively. We assume the DC electron drift velocity in the side metal contacts to be zero since $N_M \gg N_{2D}$. In this case the integrals in equation (8) can be evaluated explicitly and the free function $f(a)$ can be determined using the condition of the periodicity of the FET array with period $L$. In such a way, we can calculate the amplitudes of the oscillating 2D electron density $\tilde{N}(x) = \psi_N(x)/V_0(x)$ and electron velocity $\tilde{V}(x) = \psi_V(x)/V_0(x)$ and then obtain the oscillating current density in the plane of the FET channel $J(x,0) = e[N_0(x)\tilde{V}(x) + V_0(x)\tilde{N}(x)]$. Substituting this electric current density into Ohm's law in the form of equation (3) yields the conductivity function

$$\sigma_m(x) = \begin{cases} \sigma_m^{(1)} & \text{for } 0 \leqslant x < w/2, \\ \sigma_m^{(2)} & \text{for } w/2 \leqslant x < w, \\ \sigma_{\mathrm{M}} & \text{for } w \leqslant x < L. \end{cases} \tag{9}$$

where

$$\sigma_m^{(1,2)} = \mathrm{i}\frac{e^2 N_{2D}^{(1,2)}\omega}{m\left(\omega - q_m V_0^{(1,2)}\right)\left(\omega - q_m V_0^{(1,2)} + \mathrm{i}\nu\right)} \tag{10}$$

are the conductivities of the 2D electron channel in half-section 1 and 2 of the FET unit for different wavevectors $q_m = 2\pi m/L$, which account for the spatial dispersion of the 2D electron plasma conductivity arising due to the DC electron drift, $\sigma_{\mathrm{M}}$ is a frequency-independent conductivity of the metal side contacts. Because we assume that the DC electron drift velocity is zero in the side metal contacts, there is no spatial dispersion inherent in $\sigma_{\mathrm{M}}$ and, hence, it has the same value for all wavevectors $q_m = 2\pi m/L$. It should be noted that a simple expression, equation (10), for the conductivity function of spatially confined drifting 2D electron plasma can be obtained only for the rectangular profile of spatial modulation of the equilibrium electron density and DC drift velocity because otherwise the integrals in equation (8) cannot be taken as elementary functions.

## 2. Electromagnetic formalism

We consider a periodic sequence of 2D electron channels separated by the metal side contacts lying in the plane $y = 0$ at the surface of the substrate with dielectric constant $\varepsilon_3$ (figure 1). The metal gates are separated from the 2D electron channels by a barrier slab of thickness $d$, having dielectric constant $\varepsilon_2$. A plane electromagnetic wave with frequency $\omega$ and electric field $E(y,t) = E^{(0)}\exp(-\mathrm{i}\omega t - \mathrm{i}k_0 y)$, where $k_0 = \omega/c$, with c being the speed of light, is incident upon the structure normally from the ambient media with dielectric constant $\varepsilon_1 = 1$ (vacuum). The electric field of the incident electromagnetic wave is polarized in the direction of periodicity of the FET array (the $x$-direction).

The total electric field **E** in the structure is determined by the Maxwell equations. After Fourier transformation of the Maxwell equations and applying the conventional boundary conditions for the electric and magnetic fields at $y = 0$ and $d$, we can inter-relate the Fourier amplitudes of the oscillating in-plane electric field and currents in the 2D electron channel and gate planes:

$$\begin{aligned} E_m(d) &= Z_m^{(1,1)}J_m(d) + Z_m^{(1,2)}J_m(0) + \eta_1 E^{(0)}\delta_{m,0}, \\ E_m(0) &= Z_m^{(2,1)}J_m(d) + Z_m^{(2,2)}J_m(0) + \eta_2 E^{(0)}\delta_{m,0}, \end{aligned} \tag{11}$$

where

$$Z_m^{(1,1)} = \mathrm{i}\frac{4\pi}{\omega\Delta_m^{(1)}}\left(\beta_m^{[2,3]}\chi_m^{(2)} + \frac{\alpha_m^{[2,3]}}{\chi_m^{(2)}}\right),$$
$$Z_m^{(1,2)} = \mathrm{i}\frac{8\pi\varepsilon_2}{\omega\Delta_m^{(1)}p_m^{(2)}},$$
$$\eta_1 = \frac{1}{\Delta_0\chi_0^{(1)}}\left[\left(\alpha_0^{[2,1]}\chi_0^{(2)} + \frac{\beta_0^{[2,1]}}{\chi_0^{(2)}}\right)\left(\beta_0^{[2,3]}\chi_0^{(2)} + \frac{\alpha_0^{[2,3]}}{\chi_0^{(2)}}\right) - \left(\frac{2\varepsilon_2}{p_0^{(2)}}\right)^2\right] + \frac{1}{\chi_0^{(1)}},$$
$$Z_m^{(2,1)} = \mathrm{i}\frac{8\pi\varepsilon_2}{\omega\Delta_m^{(1)}p_m^{(2)}},$$
$$Z_m^{(2,2)} = \mathrm{i}\frac{4\pi}{\omega\Delta_m^{(1)}}\left(\beta_m^{[2,1]}\chi_m^{(2)} + \frac{\alpha_m^{[2,1]}}{\chi_m^{(2)}}\right),$$
$$\eta_2 = \frac{2\varepsilon_2}{\Delta_0 p_0^{(2)}\chi_0^{(1)}}\left(\alpha_0^{[2,1]} - \beta_0^{[2,1]}\right)\left(\chi_0^{(2)} - \frac{1}{\chi_0^{(2)}}\right),$$
$$\Delta_m^{(1)} = \frac{\chi_m^{(2)}}{1 - \left(\chi_m^{(2)}\right)^2}\Delta_m;$$

$$\Delta_m = \left[\left(\frac{2\varepsilon_2}{p_m^{(2)}}\right)^2 - \left(\beta_m^{[2,3]}\chi_m^{(2)} + \frac{\alpha_m^{[2,3]}}{\chi_m^{(2)}}\right) \times \left(\beta_m^{[2,1]}\chi_m^{(2)} + \frac{\alpha_m^{[2,1]}}{\chi_m^{(2)}}\right)\right],$$

with

$$\alpha_m^{[k,l]} = \frac{\varepsilon_k p_m^{(l)} + \varepsilon_l p_m^{(k)}}{p_m^{(k)} p_m^{(l)}}, \qquad \beta_m^{[k,l]} = \frac{\varepsilon_k p_m^{(l)} - \varepsilon_l p_m^{(k)}}{p_m^{(k)} p_m^{(l)}} \quad \begin{pmatrix} k = 1,2,3 \\ l = 1,2,3 \end{pmatrix},$$

$$\chi_m^{(1)} = \exp\left(-p_m^{(1)} d\right), \qquad \chi_m^{(2)} = \exp\left(-p_m^{(2)} d\right),$$

and

$$p_m^{(k)} = \pm\sqrt{q_m^2 - \left(\frac{\omega}{c}\right)^2 \varepsilon_k} \qquad (k = 1, 2, 3).$$

The sign before the radical in the last expression is chosen to satisfy the conditions at $y \to \pm\infty$, which are the zero field condition for the evanescent Fourier-harmonics ($m \neq 0$), and the scattering condition for the radiative Fourier-harmonics ($m = 0$). The latter condition requires that only electromagnetic waves outgoing from the FET array exist at $y \to \pm\infty$.

The amplitudes of the Fourier-harmonics of the oscillating electric current density in the 2D electron channel $y = 0$ and the gate $y = d$ planes are

$$J_m(0) = \frac{1}{L}\int_0^L J(x,0)\exp(-\mathrm{i}q_m x)\,\mathrm{d}x, \qquad J_m(d) = \frac{1}{L}\int_0^L J(x,d)\exp(-\mathrm{i}q_m x)\,\mathrm{d}x, \tag{12}$$

where $J(x,d)$ and $J(x,0)$ are the (spatially periodic with period $L$) amplitudes of the oscillating electric current densities in the FET array gates and in the 2D electron channel plane. These electric current densities are defined as

$$J(x,0) = \begin{cases} J_1(x) & \text{for } 0 < x < w/2, \\ J_2(x) & \text{for } w/2 < x < w, \\ J_C(x) & \text{for } w < x < L, \end{cases} \tag{13}$$

$$J(x,d) = \begin{cases} J_G(x) & \text{for } 0 < x < w, \\ 0 & \text{for} w < x < L, \end{cases} \tag{14}$$

where according to equation (3)

$$J_1(x) = \sum_{m=-\infty}^{\infty} \sigma_m^{(1)} E_m(0)\exp(\mathrm{i}q_m x), \tag{15}$$

$$J_2(x) = \sum_{m=-\infty}^{\infty} \sigma_m^{(2)} E_m(0)\exp(\mathrm{i}q_m x), \tag{16}$$

$$J_C(x) = \sigma_C \sum_{m=-\infty}^{\infty} E_m(0)\exp(\mathrm{i}q_m x), \tag{17}$$

$$J_G(x) = \sigma_G \sum_{m=-\infty}^{\infty} E_m(d)\exp(\mathrm{i}q_m x), \tag{18}$$

with $\sigma_m^{(1)}$ and $\sigma_m^{(2)}$ being the conductivities of the 2D drifting electron fluid in the half-sections 1 and 2 of the FET unit channel defined by equation (10) for ($V_0^{(2)} = V_0 = -V_0^{(1)}$), and $\sigma_C, \sigma_G$ are the local frequency-independent sheet conductivities of the side and gate contacts, respectively. From now on we assume that $\sigma_C$ and $\sigma_G$ have equal values $\sigma_M$.

Using Ohm's law given by equations (15)–(19), definitions from equation (12), and relationships given by equation (11) we construct the system of four coupled integral equations for the current densities in different parts of the FET unit:

$$J_1(x) = \int_0^{w/2} J_1(x')G_{1,1}(x,x')\,\mathrm{d}x' + \int_{w/2}^{w} J_2(x')G_{1,2}(x,x')\,\mathrm{d}x' + \int_w^L J_C(x')G_{1,3}(x,x')\,\mathrm{d}x' + \int_0^w J_G(x')G_{1,4}(x,x')\,\mathrm{d}x' + G_{1,0} \quad \text{for } 0 \leqslant x \leqslant w/2, \tag{19}$$

$$J_2(x) = \int_0^{w/2} J_1(x')G_{2,1}(x,x')\,\mathrm{d}x' + \int_{w/2}^{w} J_2(x')G_{2,2}(x,x')\,\mathrm{d}x' + \int_w^L J_C(x')G_{2,3}(x,x')\,\mathrm{d}x' + \int_0^w J_G(x')G_{2,4}(x,x')\,\mathrm{d}x' + G_{2,0} \quad \text{for } w/2 \leqslant x \leqslant w, \tag{20}$$

$$J_C(x) = \int_0^{w/2} J_1(x')G_{3,1}(x,x')\,\mathrm{d}x' + \int_{w/2}^{w} J_2(x')G_{3,2}(x,x')\,\mathrm{d}x' + \int_w^L J_C(x')G_{3,3}(x,x')\,\mathrm{d}x' + \int_0^w J_G(x')G_{3,4}(x',x)\,\mathrm{d}x' + G_{3,0} \quad \text{for } w \leqslant x \leqslant L, \tag{21}$$

$$J_G(x) = \int_0^{w/2} J_1(x')G_{4,1}(x,x')\,\mathrm{d}x' + \int_{w/2}^{w} J_2(x')G_{4,2}(x,x')\,\mathrm{d}x' + \int_w^L J_C(x')G_{4,3}(x,x')\,\mathrm{d}x' + \int_0^w J_G(x')G_{4,4}(x,x')\,\mathrm{d}x' + G_{4,0} \quad \text{for } 0 \leqslant x \leqslant w, \tag{22}$$

with the kernels

$$G_{1,1} = G_{1,2} = G_{1,3} = \frac{1}{L}\sum_{m=-\infty}^{\infty} \sigma_m^{(1)} Z_m^{(2,2)} \exp\left[\mathrm{i}q_m(x-x')\right],$$

$$G_{1,4} = \frac{1}{L}\sum_{m=-\infty}^{\infty} \sigma_m^{(1)} Z_m^{(2,1)} \exp\left[\mathrm{i}q_m(x-x')\right],$$

$$G_{2,1} = G_{2,2} = G_{2,3} = \frac{1}{L}\sum_{m=-\infty}^{\infty} \sigma_m^{(2)} Z_m^{(2,2)} \exp\left[\mathrm{i}q_m(x-x')\right],$$

$$G_{2,4} = \frac{1}{L}\sum_{m=-\infty}^{\infty} \sigma_m^{(2)} Z_m^{(2,1)} \exp\left[\mathrm{i}q_m(x-x')\right],$$

$$G_{3,1} = G_{3,2} = G_{3,3} = \frac{\sigma_M}{L}\sum_{m=-\infty}^{\infty} Z_m^{(2,2)} \exp\left[\mathrm{i}q_m(x-x')\right],$$

$$G_{1,4} = \frac{\sigma_M}{L} \sum_{m=-\infty}^{\infty} Z_m^{(2,1)} \exp\left[iq_m(x-x')\right],$$

$$G_{4,1} = G_{4,2} = G_{4,3} = \frac{\sigma_M}{L} \sum_{m=-\infty}^{\infty} Z_m^{(1,2)} \exp\left[iq_m(x-x')\right],$$

$$G_{4,4} = \frac{\sigma_M}{L} \sum_{m=-\infty}^{\infty} Z_m^{(1,1)} \exp\left[iq_m(x-x')\right],$$

and the free terms

$$G_{1,0} = \eta_1 E^{(0)} \sigma_0^{(1)}, \qquad G_{2,0} = \eta_1 E^{(0)} \sigma_0^{(2)},$$

$$G_{3,0} = \eta_1 E^{(0)} \sigma_M, \qquad G_{4,0} = \eta_2 E^{(0)} \sigma_M.$$

We solve integral equations (19)–(22) numerically, approximating the current densities in different parts of the FET unit by the expansions

$$J_1(\xi_1) = \sum_{n=0}^{\infty} C_n^{(1)} P_n(\xi_1), \qquad J_2(\xi_2) = \sum_{n=0}^{\infty} C_n^{(2)} P_n(\xi_2),$$

$$J_C(\xi_3) = \sum_{n=0}^{\infty} C_n^{(3)} P_n(\xi_3), \qquad J_G(\xi_4) = \sum_{n=0}^{\infty} C_n^{(4)} P_n(\xi_4), \tag{23}$$

where $P_n(\xi_{1-4})$ are the Legendre polynomials of $n$th degree and $C_n^{(1-4)}$ are unknown coefficients. Variables $\xi_{1-4}(-1 \leqslant \xi_{1-4} \leqslant 1)$ are related to the $x$-coordinate by

$$x = (1+\xi_1)w/4, \qquad (0 \leqslant x \leqslant w/2),$$

$$x = (3+\xi_2)w/4, \qquad (w/2 \leqslant x \leqslant w),$$

$$x = (3+\xi_3)w/2, \qquad (w \leqslant x \leqslant L),$$

$$x = (1+\xi_4)w/2, \qquad (0 \leqslant x \leqslant w).$$

Substituting the expansions of equation (23) into the integral equations (19)–(22) and using Galerkin's procedure [12] with the Legendre polynomials $P_n(\xi_{1-4})$ as the orthogonal basis functions, we transform the system of integral equations (19)–(22) into an infinite system of linear algebraic equations for the coefficients $C_n^{(1-4)}$, which could then be truncated and solved numerically to achieve a desired level of convergence.

Once the electric current densities given by equation (23) are found, we can calculate (using equation (12)) the amplitudes of the Fourier-harmonics of the oscillating current densities in the 2D electron channel $y = 0$ and the gate $y = d$ planes:

$$J_m(0) = l_1 \exp(-i\pi m l_1) \sum_{n=0}^{n_{max}} i^n C_n^{(1)} j_n(-\pi m l_1) + l_1 \exp(-i2\pi m l_1) \sum_{n=0}^{n_{max}} i^n C_n^{(2)} j_n(-\pi m l_1) + l_2 \exp(-i\pi m l_2) \sum_{n=0}^{n_{max}} i^n C_n^{(3)} j_n(-\pi m l_2),$$

$$J_m(d) = l_3(-1)^m \exp(-i\pi m l_3) \sum_{n=0}^{n_{max}} i^n C_n^{(4)} j_n(-\pi m l_3),$$

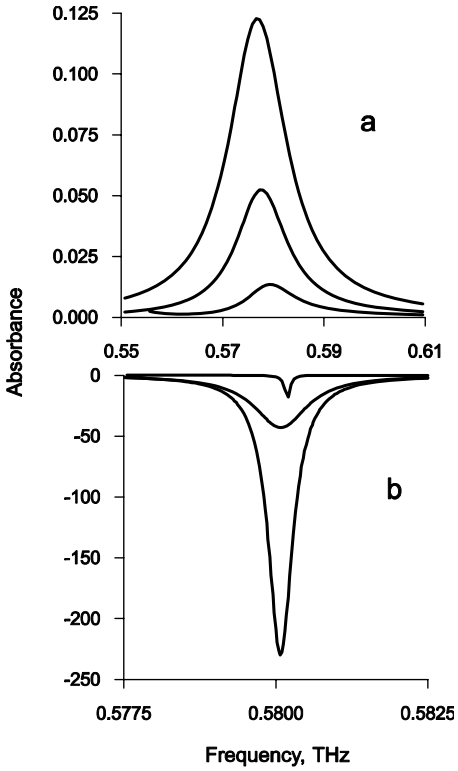


**Figure 2.** Spectra of THz (a) absorption and (b) amplification in the FET array at the fundamental plasmon resonance. Electron DC drift velocities in the FET channel are (from the top to bottom): $1 \times 10^4$, $4 \times 10^5$, $5.5 \times 10^5$, $1 \times 10^6$, $1 \times 10^7$, $7.35 \times 10^6$ cm s$^{-1}$. Other FET parameters are $N_{2D} = 2.57 \times 10^{11}$ cm$^{-2}$, $\nu = 1.5 \times 10^{10}$ s$^{-1}$, $L = 4$ $\mu$m, $w = 2$ $\mu$m, $d = 0.4$ $\mu$m, $m = 0.067m_0$, where $m_0$ is the free electron mass.

where $l_1 = w/(2L)$, $l_2 = 1 - w/L$, $l_3 = w/L$, and $j_n(\vartheta)$ is the spherical Bessel function of the first kind of the $n$th order. These amplitudes of the Fourier-harmonics of the oscillating current density are then used to calculate the electric fields by equation (11).

The absorbance, $A$, of the FET array is calculated by the Joule law

$$A = \frac{1}{2LP_0} \mathrm{Re}\left[\int_0^{w/2} J_1^*(x)E(x,0)\,dx + \int_{w/2}^{w} J_1^*(x)E(x,0)\,dx + \int_w^L J_C^*(x)E(x,0)\,dx + \int_0^w J_G^*(x)E(x,d)\,dx\right], \tag{24}$$

where $P_0 = c|E^{(0)}|^2/8\pi$ is the energy flux density in the incident wave ($A > 0$ in the absorption regime and $A < 0$ in the amplification regime). We can also calculate the reflectance, $R$, and transmittance, $T$, of the FET array as $R = |E_0(d)|^2/|E^{(0)}|^2$ and $T = |E_0(0)|^2\sqrt{\varepsilon_3}/|E^{(0)}|^2$, respectively. In both the absorption and amplification regimes the energy conservation law, $A + R + T = 1$, is satisfied.

## 3. Results and discussion

Figure 2 shows the evolution of the THz absorption spectrum of the FET array at the fundamental plasmon resonance when the DC electron drift velocity/bias current in each section

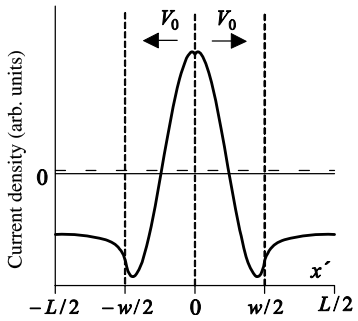


**Figure 3.** Oscillating current density over the period of the FET array at the fundamental plasmon resonance for the DC drift velocity $7.35 \times 10^6$ cm s$^{-1}$. The horizontal dashed line marks the amplitude of the current excited in a side contact by the incoming uniform THz wave. $x' = x - w/2$.

of the FET unit increases. At small DC bias current, the plasmon absorption resonance decreases in intensity, becoming narrower because of decreasing the radiative linewidth of the plasmon resonance. At a certain threshold value of the DC drift velocity, the absorption becomes negative, which corresponds to the amplification of the incoming THz wave (either the THz reflection or transmission coefficients are greater than unity). The width of the amplification line is by an order of magnitude less than the plasmon absorption linewidth because, in the former case, the dissipation linewidth and the radiation linewidth of the unstable plasmons (which is negative in the amplification regime) cancel each other (pay attention to different scales along the frequency axis in figures 2(a) and (b)).

Distribution of the oscillating current density over the FET unit at the fundamental plasmon resonance in the amplification regime (figure 3) has an even symmetry in respect to the center of the FET unit (this corresponds to an odd symmetry of the distribution of the vertical component of the oscillating electric field with its node in the center of the FET unit). It follows from figure 3 that even at the fundamental plasmon resonance half of the plasmon wavelength is shorter than the length of the gate contact of the FET unit, while in a single-gate FET with symmetrical boundary conditions at different ends of the gated region of the channel half of the plasmon wavelength exceeds the length of the gate contact due to the effect of fringing fields [9]. This happens because the plasmon oscillations in the FET array are more 'rigid' due to the effect of the side metal contacts connecting different FET units. Inhomogeneous currents forming the standing plasmon mode in the FET unit oscillate under the gate contact and at the edges of the side contacts, while a homogeneous oscillating current flows in the middle part of a side contact. This homogeneous current is defined by the current excited in a side contact by the incoming uniform THz wave and the induced current excited in a side contact by plasmon charges oscillating at the edges of the side contact.

In accordance with [2], the amplification develops at small DC drift velocities $V_0/V_{\rm ph} < 1$, where $V_{\rm ph}$ is the plasmon phase velocity. The plasmon phase velocity at the fundamental plasmon resonance is $V_{\rm ph} = \lambda_p \omega/2\pi$, where $\lambda_p$ can be estimated as a double distance between the two antinodes in figure 3. However, the strongest amplification, with the highest amplification factor exceeding 200, takes place at much smaller DC drift velocities $V_0/V_{\rm ph} \ll 1$, which correspond to drain currents much smaller than the saturation current, than those ensuring the largest plasmon instability increments predicted in [2]. The reason for this is that the condition for the plasmon instability and the condition for optimal coupling of the unstable plasmons to THz radiation differ so that smaller THz amplification is reached under stronger plasmon instability.

## 4. Conclusions

In conclusion, we have shown that the FET array with additional contacts under the centers of the gates can effectively amplify THz radiation via the hydrodynamic plasmon instability mechanism even at small drain DC currents, far below the saturation current regime. No special antenna elements are needed to couple the unstable plasmons to THz radiation because the FET array itself acts as an effective aerial matched receiving/emitting antenna. No special lumped circuit element design is needed to ensure specific boundary conditions in the ends of the FET channel, which are necessary for the conventional plasmon instability. Such conditions are automatically satisfied by the excitation of the plasmon mode with proper symmetry in the FET unit by incoming THz radiation, while the FET array has an entirely planar design. This makes FET arrays very attractive for potential applications as THz emitters and amplifiers.

## Acknowledgments

This work has been supported by the Russian Foundation for Basic Research (grant 06-02-16155) and the Russian Academy of Sciences program 'Quantum Nanostructures'. MSS acknowledges a support from the Office of Naval Research and from the National Science Foundation under the auspices of the I/UCRC 'Connection One'.

## References

[1] Shur M S and Lü J-Q 2000 *IEEE Trans. Microw. Theory Tech.* **48** 750
[2] Dyakonov M I and Shur M S 1993 *Phys. Rev. Lett.* **71** 2465
[3] Knap W, Lusakowski J, Parenty T, Bollaert S, Cappy A, Popov V V and Shur M S 2004 *Appl. Phys. Lett.* **84** 2331
[4] Otsuji T, Hanabe M and Ogawara O 2004 *Appl. Phys. Lett.* **85** 2119
[5] Dyakonova N, El Fatimy A, Łusakowski J, Knap W, Dyakonov M I, Poisson M-A, Morvan E, Bollaert S, Shchepetov A, Roelens Y, Gaquiere Ch, Theron D and Cappy A 2006 *Appl. Phys. Lett.* **88** 141906
[6] Matov O R, Meshkov O F, Polischuk O V and Popov V V 1997 *Physica* A **241** 409–13
[7] Mikhailov S A and Savostianova N A 1997 *Appl. Phys. Lett.* **71** 1308
[8] Mikhailov S A 1998 *Phys. Rev.* B **58** 1517
[9] Popov V V, Polischuk O V and Shur M S 2005 *J. Appl. Phys.* **98** 033510
[10] Dyakonov M I and Shur M S 1995 *Appl. Phys. Lett.* **67** 1137
[11] Popov V V, Tsymbalov G M, Fateev D V and Shur M S 2006 *Appl. Phys. Lett.* **89** 123504
[12] Korn G and Korn T 1968 *Mathematical Handbook for Scientists and Engineers* 2nd edn (New York: McGraw-Hill)